International Journal of Frontiers in
Engineering and Technology Research
Journal homepage: https://frontiersrj.com/journals/ijfetr/
ISSN: 2783-0497 (Online)

(REVIEW ARTICLE)

WR21 marine gas turbine thermodynamic simulator for ship propulsion studies

Ugo Campora *

Department of Mechanical, Energy, Management and Transportation Engineering, Polytechnic School, University of Genoa, Genoa, Italy.

International Journal of Frontiers in Engineering and Technology Research, 2024, 06(01), 001–015

Publication history: Received on 09 December 2023; revised on 27 January 2024; accepted on 30 January 2024

Article DOI: https://doi.org/10.53294/ijfetr.2024.6.1.0023

Abstract

An original modular mathematical model, based on physical laws, for steady state and dynamics performance simulation of the WR21 gas turbine is presented in the paper. The model, developed in Matlab-Simulink language, is organized in modular form. Each gas turbine component (i.e. compressor, turbine, combustor, heat exchanger) is modelled in a specific simulator block, that simulates the performance of its pertinent component by means of steady state performance maps and/or correlations, time dependent momentum, energy and mass equations, nonlinear algebraic equations. The great application flexibility of the component simulator modules, allows to modelling any gas turbine layout (i.e. axial or radial flow compressor and turbine, rotating shafts number, heat exchangers).

The WR21gas turbine, developed mainly for marine propulsion application, is a three shafts gas turbine with thermal regeneration. It is characterized by a high thermodynamic efficiency, which remains high up to 30% of the design power.

The WR21 simulator results are validated by comparison with manufacturer or literature data. The WR21 gas turbine main performances are compared to those of the LM 2500 gas turbine, obtained by a previously author paper. The LM 2500 is the gas turbine currently most used in naval propulsion plants. In the article, a comparison between the steady state working data of the two gas turbines is reported in tabular and graphical form and commented.

Keywords: Simulation; Marine gas turbine; Intercooled recuperated gas turbine; Marine propulsion engine

1. Introduction

The gas turbine (GT) is characterized by a reduced weight-dimensions/power ratio, compared to other thermal engines, such as: steam plants and internal combustion engines. The latter, in two and four-stroke diesel versions, are currently preferred as prime movers in marine propulsion, due to the best compromise that they offer in terms of smaller size (compared to steam plants) and greater efficiency (compared to GTs). Regarding the GTs, their use in the merchant and passenger navy is practically nil. In the marine propulsion field, to remedy the GTs lower efficiency, compared to diesel engines one, plant solutions called COmbined Gas And Steam (COGAS) have been proposed in literature [1-4], which combine a GT with a bottoming steam plant, whose thermodynamic cycle is powered (thermally) by the GT Brayton cycle waste heat. In [5,6] this solution is proposed for container ship propulsion, while for passenger cruise ships and fast ferry this solution is examined in [7,8]. More recently, COGAS propulsion systems installation in Royal Caribbean's ship Radiance of the Seas, and Celebrity Cruise's ships Millennium and Infinity are reported in [9].

Due its less dimensions and weight, the GT is used as prime mover in most naval propulsion systems [10,11], being in these vessels type of minor importance the GT lower efficiency, and consequent higher fuel cost, compared to diesel engines.

* Corresponding author: Ugo Campora

The conventional GTs obtains they maximum efficiency at maximum load condition (Maximum Continuous Rating (MCR)); said efficiency decreases rapidly as the load decreases. The WR21 GT has been specifically developed to overcome this GTs defect [12,13], using the Brayton cycle thermal regeneration technique, this solution, together with the compression intercooling, also increases the overall GT thermodynamic efficiency value [12-14].

The WR21-ICR GT simulator is developed stating to the LM 2500 GT mathematical model, developed by the author [15]. The GT model is written in Matlab-Simulink language and is organized in modular form. Each GT component (i.e. compressor, combustor, turbine) is modelled in a specific simulator module.

After the WR21 simulator development and setting, its results validation is carried out by comparison between GT model ones and data reported in literature, regarding both design and off-design WR21 GT working conditions. In the article the WR21 performance and thermodynamic cycle data are compared with the analogues one, obtained from the LM 2500 GT simulator, also described and validated in [15].

2. WR21 gas turbine

As shows in the scheme of Fig. 1, the WR21-ICR (InterCooler Recuperated) GT is a three shafts, two compressors and three turbines device. An intercooler (INT in Fig. 1) is placed between the two compressors (LPc and HPc in figure). The high and low pressure turbines (HP_T and LP_T respectively in Fig. 1) are fixed blades type ones, while the power turbine (P_T in figure) is a Variable Area Nozzle blades (VAN) one [16]. After the power turbine, a cycle regenerator heat exchanger (REG in Fig. 1) preheats the air leaving the high-pressure compressor (HPc) before it enters to the combustor (Co).

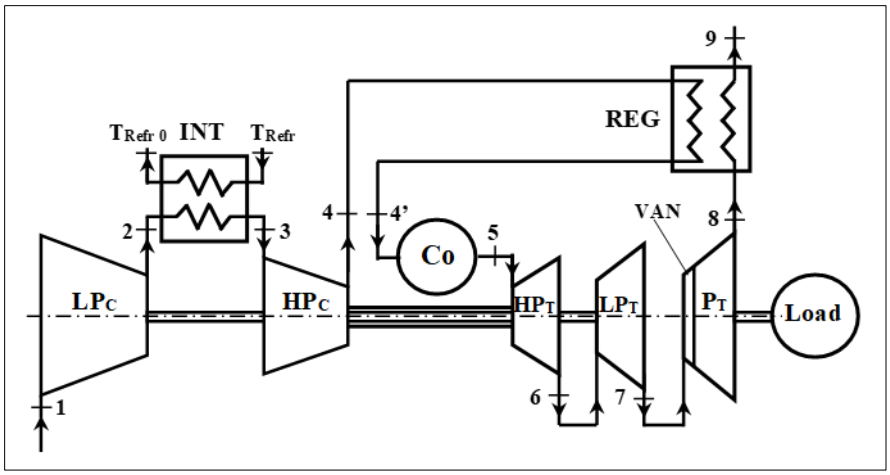

Figure 1 WR21-ICR gas turbine scheme

3. WR21 gas turbine simulator description

The WR21 GT simulator, developed in Matlab-Simulink© language, is developed starting to an also presented LM 2500 GT author simulator [15], whose basic approach is the intercomponent volumes method [17-20]. The WR21 GT model is organized in modular arrangement. Each module simulates the pertinent GT plant component by means of tabular data, correlations, steady-state and dynamic equations. Fig. 2 shows the overall WR21 GT Simulink model scheme; the figure reports the input/output parameters exchanged between the simulator modules.

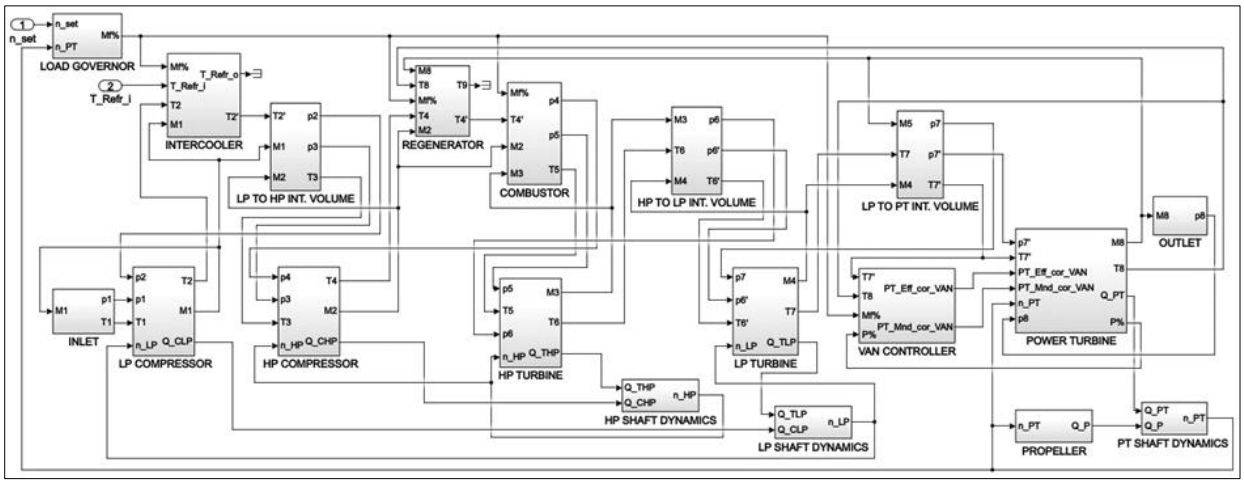

Figure 2 WR21-ICR gas turbine simulator Simulink scheme

The GT simulator basic features are

- One-dimensional flow;
- For the fluid model the ideal gas equation is used, specific energy and enthalpy are function of temperature and, for flue gas, also of gas composition [21], for the liquid, saturated enthalpy is function of the temperature and, in the liquid mixture, also to the mixture components mass percentage composition;
- Distributed parameters process is simulated as lumped parameters scheme by control volumes;
- Metal walls thermal capacity is not considered;
- Dynamic and thermodynamic parameters are time dependent;
- In the compressors, turbines and heat exchangers modules energy and mass accumulation is neglected;

The basic model modules are:

- Compressor;
- Turbine;
- Van controller;
- Combustor and intermediate volume;
- Heat exchanger;
- Shaft dynamics;
- Inlet and outlet;
- Propeller;
- Load governor.

The modules: compressor, turbine, combustor and intermediate volume, shaft dynamics, inlet and outlet, have been developed starting from the analogous ones already presented in [15], all the other modules are of new conception.

3.1. Compressor modules

In the low and high pressure compressors modules (LP compressor and HP compressor in Fig. 2) the input-output parameters are:

Inputs: stagnation inlet and outlet pressure (p), stagnation inlet temperature (T_i) and shaft speed (n).

Outputs: stagnation outlet temperature (T_o), outlet air mass flow rate (M) and shaft torque (Q_C).

In the LP and HP compressors Simulink modules of Fig. 2, steady state performance maps are used to modelling these components, by two 2D matrix [22]. The non-dimensional mass flow rate ($M_{C\,nd}$):

$$M_{Cnd} = M_C \frac{\sqrt{T_i}}{p_i} \quad \text{.....(1)}$$

and the isentropic efficiency (η_C) are expressed, both functions of the compressor pressure ratio ($\beta = p_o/p_i$) and non-dimensional shaft speed ($n_{nd} = n/\sqrt{T_i}$).

The effective outlet temperature (T_o) is given by:

$$T_o = T_i \left[1 + \frac{1}{\eta_C} \left(\beta^{\frac{\gamma-1}{\gamma}} - 1 \right) \right] \quad \text{..... (2)}$$

where γ is the ratio of specific heats (c_p/c_v).

By equation (1) the compressor mass flow rate (M_C) is obtained. The compressor shaft torque (Q_C) is then determined with:

$$Q_C = \frac{M_C \, c_p \left(T_o - T_i \right) \cdot 60}{2\pi \, n} \quad \text{..... (3)}$$

being shaft speed (n) expressed in rpm.

3.2. Turbine modules

The performance of these GT components is determined in similar way to the compressors; steady state maps [22] are used.

The input-output parameters of this modules are (Fig. 2):

Input: stagnation inlet and outlet pressure (p_i and p_o respectively), stagnation inlet temperature (T_i), shaft speed (n); further power turbine module ('power turbine' module in Fig. 2) inputs are: overall power turbine efficiency correction from 'van controller' module ($PT\ eff_{cor\ VAN}$), overall power turbine non-dimensional mass flow rate 'van controller' correction ($PT\ M_{nd\ cor\ VAN}$).

Output: stagnation outlet temperature (T_o), mass flow rate (M_T), shaft torque (Q_T); further power turbine module output is (Fig. 2): power turbine delivered power percentage ($P_{\%}$), referring the GT MCR load condition one.

Also in the turbine Simulink modules (Fig. 2), the steady state performance maps [22] are given in 2D matrix form. The non-dimensional mass flow rate ($M_{T\,nd}$):

$$M_{T\,nd} = M_T \frac{\sqrt{T_i}}{p_i} \quad \text{.....(4)}$$

and the isentropic efficiency (η_T) are both functions of the overall turbine pressure ratio ($\varepsilon = p_i/p_o$)

and of the non-dimensional shaft speed ($n_{nd} = n/\sqrt{T_i}$):

$$M_{T\,nd} = f(\varepsilon, n_{nd}) \quad \text{.....(5)}$$

$$\eta_T = f'(\varepsilon, n_{nd}) \quad \text{..... (6)}$$

The effective outlet temperature (T_o) of the expansion is determined by:

$$T_o = T_i \left[1 - \eta_T \left(1 - \varepsilon^{\frac{\gamma-1}{\gamma}} \right) \right] \text{ ..... (7)}$$

The turbine mass flow rate (M_T) is expressed by equation (4), while with equation:

$$Q_T = \frac{M_T \, c_p \left(T_i - T_o \right) \cdot 60}{2\pi \, n} \text{ .....(8)}$$

the turbine shaft torque (Q_T) is determined.

3.3. VAN controller module

The input-output parameters of this module are (Fig. 2):

Input: power turbine stagnation inlet (T_i) and outlet (T_o) temperature, GT combustor fuel mass flow rate percentage (M_f %), power turbine delivered power percentage (P %).

Output: overall power turbine efficiency correction from 'van controller' module ($PT\ eff_{cor\ VAN}$), overall power turbine non-dimensional mass flow rate 'van controller' correction ($PT\ M_{nd\ cor\ VAN}$).

The WR21 power turbine (PT in Fig. 1) is a six stage one, the first with Variable Area Nozzle (VAN) [23,24]. The 'van controller' module of Fig. 2 control the VAN nozzle area value in order to maintain constant the PT inlet stagnation temperature (T7 and T7' in Figs. 1 and 2 respectively) from full to low PT power, as reported in [24]. The VAN nozzle area value change the overall power turbine isentropic efficiency (η_T) and the non-dimensional mass flow rate ($M_{T\,nd}$) as reported in [24,25].

In the 'van controller' module a PT efficiency and the non-dimensional mass flow rate first correction factors (($PT\ eff_{cor\ VAN}$ and $PT\ M_{nd\ cor\ VAN}$ respectively) are generated as function of the combustor fuel mass flow rate percentage ($M_{f\,\%}$), that is a 'van controller' module input (Fig. 2). These correction factors values are after adjusted by two PI governor to obtain the desired PT inlet stagnation temperature values (T7' in Fig. 2), that are a VAN module input.

Similarly to the LP and HP turbine, the PT Simulink modules (Fig. 2), employ the same approach based on the steady state performance maps [22] given in 2D matrix form, where the non-dimensional mass flow rate ($M_{PT\,nd}$) and the isentropic efficiency (η_{PT}) are both functions of the overall turbine pressure ratio ($\varepsilon = p_i/p_o$), the non-dimensional shaft speed ($n_{nd} = n/\sqrt{T_i}$), eq. (5) and (6). In the 'power turbine' module the van controller effect is considered using the non-dimensional mass flow rate 'van controller' module correction factor ($PT\ M_{nd\ cor\ VAN}$ in Fig. 2), for the original map non-dimensional mass flow rate correction, and the 'van controller' module PT efficiency correction factor ($PT\ eff_{cor\ VAN}$, in the same figure), to the isentropic efficiency correction. For the PT the eqs. (5) and (6) are corrected as follows, respectively:

$$M_{PT\,nd} = f\left(\varepsilon, n_{nd}, PT\ M_{nd\ cor\ VAN}\right) \text{.....(9)}$$

$$\eta_{PT} = f'(\varepsilon, n_{nd}, PT\ eff_{cor\ VAN}) \text{ .....(10)}$$

As reported in [24], in the simulator the VAN area is fully open at PT 100% power, and fully closed (minimum area) at 40% one.

3.4. Combustor and intermediate volume modules

The variables and parameters considered in these modules are:

State variables: stagnation pressure (p) and total specific internal energy (u) of the plenum.

Input: fuel mass flow rate percentage (M_f%, in the 'combustor' block only, Fig. 2), stagnation inlet gas temperature (T_i), inlet and outlet gas mass flow rates (M_i and M_o respectively).

Output: stagnation inlet and outlet pressures (p_i and p_o respectively) and stagnation outlet temperature (T_o).

The GT combustor ('combustor' block in Fig. 2) is modelled as an adiabatic capacity, taking into account the time-dependent accumulation of mass and energy equations, respectively:

$$\frac{dp}{dt} = \frac{\gamma RT}{V}\left(M_i + M_f - M_o\right) \quad \text{..... (11)}$$

$$\frac{du}{dt} = \frac{1}{\rho V}\left(M_i h_i - M_o h_o\right) + M_f LHV \eta_b \quad \text{..... (12)}$$

with: R the gas constant; T and V the plenum gas temperature and volume respectively; ρ the gas density in the plenum; h_i and h_o the inlet and outlet gas specific enthalpy respectively; LHV the fuel lower specific value and η_b the combustor efficiency.

The combustor plenum state variables: stagnation pressure (p) and total specific internal energy (u) are determined by dynamic equations (11) and (12) respectively.

In the 'combustor' module of Fig. 2, stagnation outlet pressure and temperature (p_5 and T_5 respectively in figure) are determined by the equations:

$$p_5 = p \quad \text{.....(13)}$$

$$T_5 = \frac{u}{c_v} \quad \text{.....(14)}$$

The total pressure loss across the combustor (Δp_{cb}) id determined as function of the plenum quadratic flow velocity by:

$$\Delta p_{co} = K_{cb\,loss}\left(\frac{M_o}{\rho \Omega_{co}}\right)^2 \quad \text{.....(15)}$$

where: $K_{co\,loss}$ is the combustor friction loss coefficient, and Ω is the cross-sectional area.

The inlet combustor pressure (p_4 in the 'combustor' block of Fig. 2) is calculated by:

$$p_4 = p_5 + \Delta p_{co} \quad \text{.....(16)}$$

As reported in [15], in the GT without thermal regeneration, the 'combustor' module is naturally allocated between the HP compressor and HP turbine simulator modules, as required by the input-output parameters organisation. In the 'compressor' and 'turbine' modules, the pressure values are requested as inlet flow section input parameters, while at outlet flow sections the mass flow rates are calculated as output parameters. The contrary happens in the 'combustor' module where the pressures and the mass flow rate parameters assume an opposite role.

To this reason is not possible to connect in series two 'compressor' or 'turbine' modules, without interconnecting them to a 'combustor' one (named in Fig. 2 'intermediate volume').

The 'intermediate volume' modules calculation scheme is very similar to that used for the 'combustor' one, in this case the fuel mass flow rate (Mf) is not considered in the input variables (Fig. 2), and in the dynamic mass and energy equations (11) and (12) its value is put zero.

3.5. Heat exchanger modules

Two counterflowheat exchanger modules are employed in the GT, the 'intercooler' module in the Simulink model (Fig. 2, 'INT' in the GT scheme of Fig. 1) and the 'regenerator' module in Fig. 2 ('REG' in Fig. 1). The first is located between the LP and HP compressors, the second between the power turbine outlet and the combustor inlet (Fig. 1). These modules are modelled in very similar manner.

The input-output variables of these modules are:

Input: fuel mass flow rate percentage ($M_{f\%}$), refrigerant fluid stagnation inlet temperature ($T_{refr\,i}$), cooled fluid stagnation inlet temperature ($T_{co\,i}$), refrigerant fluid inlet mass flow rate ($M_{refr\,I}$, in the 'regenerator' module only), cooled fluid inlet mass flow rate ($M_{co\,i}$).

Output: stagnation refrigerant and cooling fluids outlet temperature ($T_{refr\,o}$ and $T_{co\,o}$ respectively).

The thermal flows (Φ) exchanged in both modules are determined with the same simple approach, that employ the heat exchangers efficiency (ε), defined by equation:

$$\varepsilon = \frac{\Phi_{effect\ exch}}{\Phi_{theor\ exch}} = \frac{M_{co\,i}\left(h_{co\,i} - h_{co\,o}\right)}{M_{co\,i}\left(h_{co\,i} - h_{refr\,i}\right)} = \frac{M_{refr\,i}\left(h_{refr\,o} - h_{refr\,i}\right)}{M_{refr\,i}\left(h_{co\,i} - h_{refr\,i}\right)} \quad \text{..... (17)}$$

with the constrain:

$$\Phi_{co\ effect\ \ exch} = \Phi_{refr\ effect\ \ exch} \quad \text{.....(18)}$$

In equations (17) and (18): $\Phi_{effect\ exch}$ and $\Phi_{theor\ exch}$ are the effective and theoretical heat flow exchanged; $h_{co\,i}$ and $h_{co\,o}$ are the cooling fluid inlet and outlet specific enthalpy respectively; $h_{refr\,i}$ and $h_{refr\,o}$ are the refrigerant fluid inlet and outlet specific enthalpy respectively; $\Phi_{co\ effect\ exch}$ and $\Phi_{refr\ effect\ exch}$ are respectively the effective heat flow exchanged between cooling and refrigerant fluids.

In equation (17) the heat exchangers efficiency (ε) value is variable as function of the GT load. In the 'intercooler' module, from the data reported in [23,26,27], its value is increased from about 84% at GT full load to about 92% at 30% load. The coolant fluid is a 50/50 mixture of water and glycol. The regenerator efficiency is varied between about 85% at full load and about 89% to 30% one [26,28]. In the Simulink model, for both heat exchangers, the fuel mass flow rate percentage ($M_{f\%}$ in Fig. 2) value is defined in the 'load governor' module. In both heat exchanger modules, the fluid pressure losses between inlet and outlet are neglected.

3.6. Shaft dynamics modules

The GT shafts rotational speed time variation are determined in this block type.

In these modules the input and output variables are (Fig. 2):

Input: turbine torque (Q_T), compressor or propeller torque (Q_C or Q_P respectively).

Output: shaft rotational speed (n).

In the module the shaft speed (n) is determined by the dynamic shaft equation:

$$\frac{dn}{dt} = \frac{1}{J \cdot 2\pi}\left(Q_T - Q_{br}\right) \quad \text{..... (19)}$$

where: J is the rotor inertia; Q_T the turbine torque; Q_{br} the brake torque (compressor or propeller torque).

3.7. Inlet and outlet modules

The GT inlet and outlet ducts pressure losses are determined in these two blocks, where the ambient conditions: stagnation ambient pressure (p_a) and temperature (T_a) are provided as constant values.

The 'inlet' module (Fig. 2) input and output parameters are:

Input: low pressure compressor mass flow rate (M_1).

Output: outlet duct stagnation pressure and temperature (p_o and T_o respectively).

By equation:

$$p_o = p_a - \Delta p_{in\,loss} \quad \text{.....(20)}$$

the stagnation outlet pressure (p_o) is determined, where $\Delta p_{in\,loss}$ is the total pressure loss across the GT inlet duct, an equation similar to (15) is employed to calculate this parameter. The outlet section stagnation temperature is determined by the simple equation:

$$T_o = T_a \quad \text{.....(21)}$$

In the GT simulator 'outlet' module of Fig. 2, the input and output parameters are:

Input: inlet section mass flow rate (M_8).

Output: inlet section stagnation pressure (p_8), being neglected the 'regenerator' fluids pressure loss.

In this module, its inlet section stagnation pressure is evaluated by:

$$p_i = p_a + \Delta p_{out} \quad \text{.....(22)}$$

where the total pressure loss across the GT power turbine outlet duct (Δp_{out}) is determined with equation like (15).

3.8. Propeller module

In the 'propeller' module (Fig. 2), the propeller torque vs PT shaft speed law [28] is adopted. The input and output of this block are:

Input: PT shaft rotational speed (n_{PT}).

Output: propeller torque (Q_P), that include the overall shaft line mechanical loss.

3.9. Load governor module

The GT delivered power and torque (from the 'power turbine' module, Fig. 2) is defined by the 'load governor' block, whose inputs and outputs are:

Input: PT shaft required and effective rotational speed (n_{set} and n_{PT} respectively).

Output: fuel mass flow rate percentage ($M_{f\%}$).

The load governor module manages the combustor fuel mass flow rate percentage (referring to the GT full power one), by a PI governor, to obtain the required PT speed (n_{PT}), and as consequence the PT delivered torque (Q_{PT} from the 'power turbine' block of Fig. 2).

4. Model application and validation

Tab. 1 reports the main WR21-ICR GT design (MCR) data [28]. The WR21 GT simulator modules have been set up on the data reported mainly in [28] and in [12,23,24,29]. In the table *BSFC* is the GT Brake Specific Fuel Consumption.

Tab 2 shows, as percentage difference, the difference between simulator and reference data, referring the main GT main components, referred to GT design (MCR) working condition. The percentage difference ($\Delta x/x\%$) values reported in the table are determined by:

$$\Delta x/x\% = \frac{x_{sim} - x_{ref}}{x_{ref}} 100 \ [\%] \quad \text{.....(23)}$$

with: x_{sim} and x_{ref} are the generic variables referred to GT simulator and reference respectively.

Table 1 WR21-ICR GT MCR data

GT parameter	**value**
delivered power [MW]	25.2
PT speed [rpm]	3600
overall compression ratio (β_{GT})	14.2
combustor outlet temperature (T_5) [°C]	1500
PT inlet temperature (T_7) [°C]	852
BSFC [g/kWh]	219.1

Table 2 WR21-ICR GT MCR load condition main parameters validation

GT component	**parameter**	**difference [%]**
LP compressor	pressure ratio ($\beta_{LP\,C}$)	0.14
	inlet temperature (T_1)	0.00
	outlet temperature (T_2)	0.37
HP compressor	pressure ratio ($\beta_{HP\,C}$)	0.08
	inlet temperature (T_3)	0.17
	outlet temperature (T_4)	0.34
regenerator	cold air outlet temperature ($T_{4'}$)	-0.07
	hot gas outlet temperature (T_9)	0.20
combustor	fuel mass flow rate (M_f)	0.08
	outlet temperature (T_5)	-0.89
HP turbine	rotational speed (n_{HP})	0.20
LP turbine	rotational speed (n_{LP})	0.21
power turbine	inlet temperature (T_7)	0.00
	outlet temperature (T_8)	-0.10
	delivered power	0.00
overall GT	overall pressure ratio (β_{GT})	0.27
	BSFC	-0.90

Data reported in Tab. 2 shows a very good agreement between GT model and reference data, difference is generally less to 0.4%, and only for two parameters reach 0.9%.

To WR21 GT model results off-design validation, the GT PT load versus speed, reported in Fig. 3 [29], is adopted. This law is referred to a ship variable pitch propeller characteristic [28].

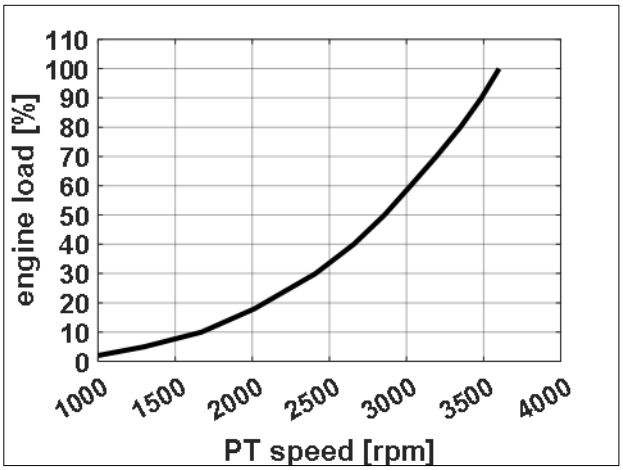

Figure 3 WR21 GT load-speed curve from a ship variable pitch propeller one

Fig. 4a and 4b reports, in the LP and HP compressors performance maps respectively, the compressor working conditions trajectory from 100% to 10% MCR engine load. Figure shows a very good agreement between GT model and reference data [13]. In the LP compressor, the working line curvilinear shape (Fig. 4a) is due to the VAN action effect, as reported in [12,29].

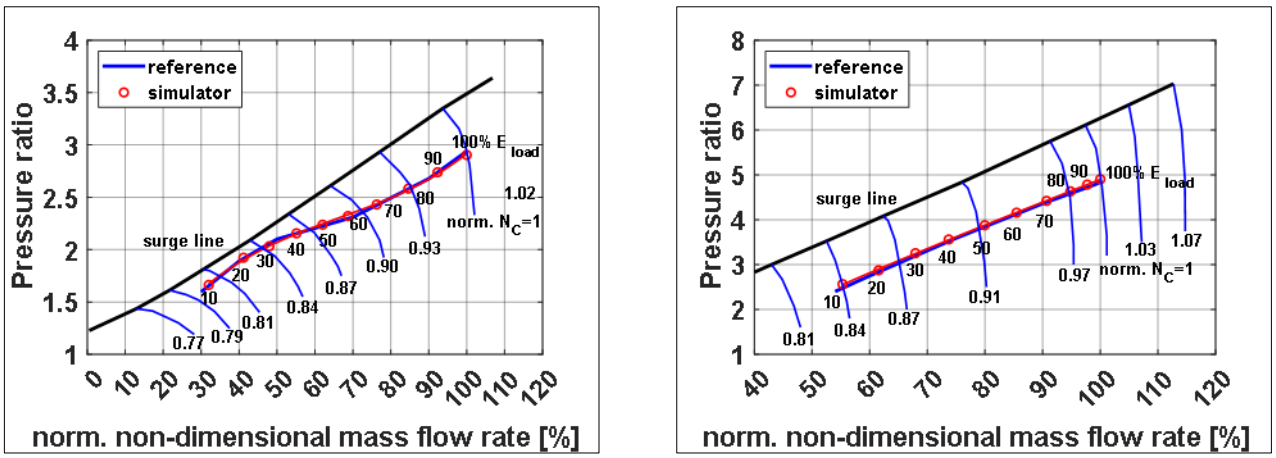

a b

Figure 4 WR21 GT simulator working line in the LP (a) and HP (b) compressor vs GT load and comparison with reference data

Fig. 5 a and b shows respectively the combustor outlet temperature and the GT Brake Specific Fuel Consumption (BSFC), both vs engine load, and the comparison with reference data, [29] for Fig. 5a and [28] for Fig. 5b, also for these parameters can be observed a good agreement between GT model results and reference data.

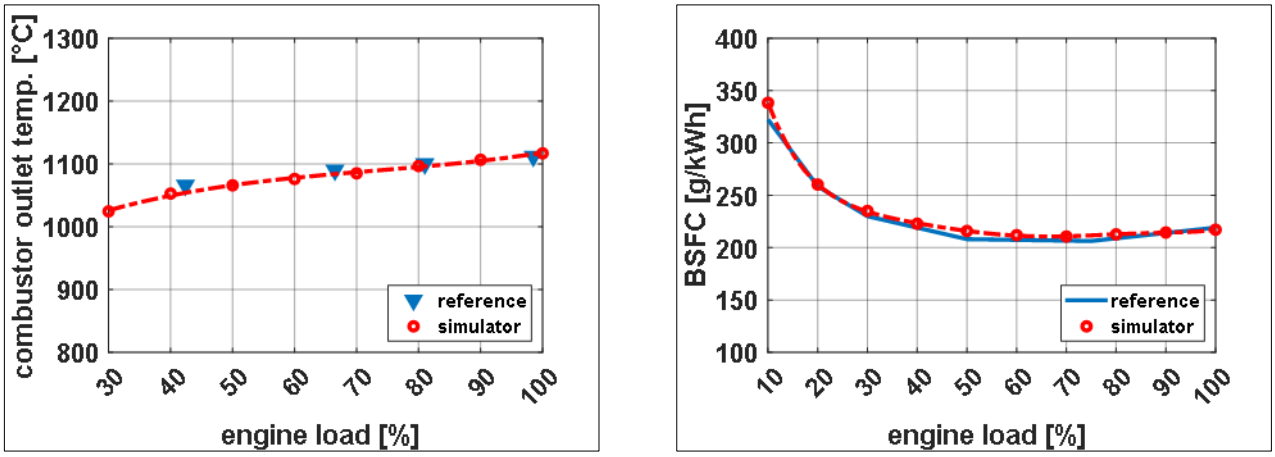

a b

Figure 5 WR21 GT simulator combustor outlet temperature (a) and BSFC (b) vs GT load and comparison with reference data

5. Comparison with LM 2500 GT

In this article section the main WR21 data and their variation with engine load is compared to the analogues one of the LM2500 GT, the most gas turbine type used in naval propulsion plants. The LM2500+G4 version is used for the comparison, having the authors already developed and validated its simulation model in a previously paper [15]. The LM2500+G4 is a two shaft GT, the first is the gas generator (comprising: compressor, combustor), the second shaft is pertinent the HP turbine, that move the propeller through a reduction gear. The main design (MCR) characteristics of this GT are: 32 MW of PT delivered power at 3600 rpm, 1430 °C of maximum cycle temperature and 36.9% of GT efficiency.

Fig. 6a reports the combustor outlet temperature variation vs load of the two GT, figure shows that the WR21 GT has a greater temperature and its value decrease much less than the LM 2500 one.

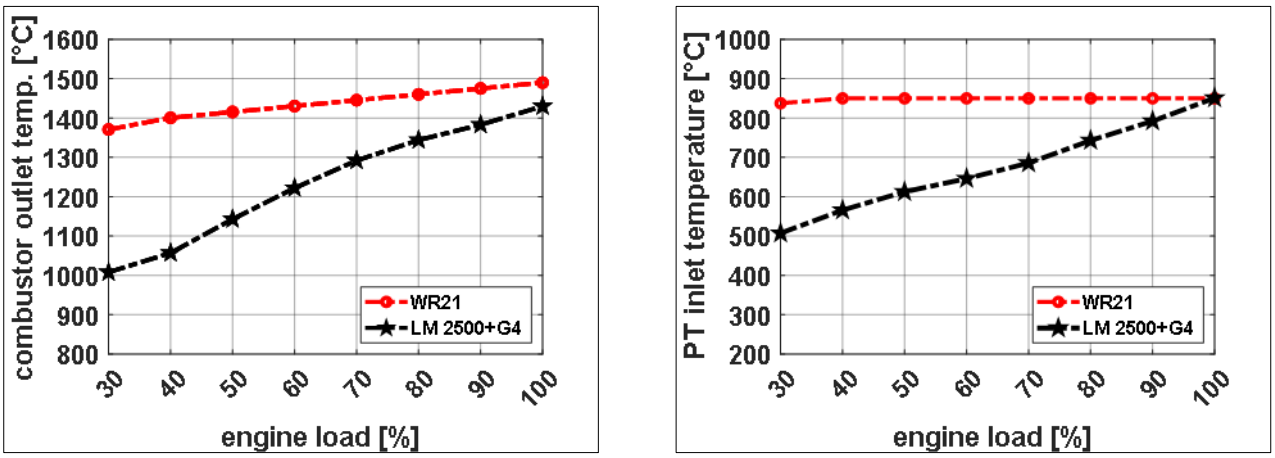

a b

Figure 6 WR21 and LM2500 GTs combustor outlet temperature (a) and PT inlet one (b) simulators results vs engines load

This difference between the two GT is due to WR21 variable section VAN action, that maintain almost constant the PT inlet temperature to load variation (Fig. 6b), while this parameter strongly decrease in the LM2500 GT, as shows in Fig. 6b.

On the contrary, Fig. 7a shows that the LM2500 compressor inlet mass flow decrease slightly to the engine load decrease, referring the WR21 one, while the overall compression ratio (much greater in the LM2500 than in the WR21,

as reported in Fig. 7b) decrease in similar manner to engine load decrease (7.7 bar from 100 to 30% MCR load the WR21, 8.8 bar in the LM2500 GT)

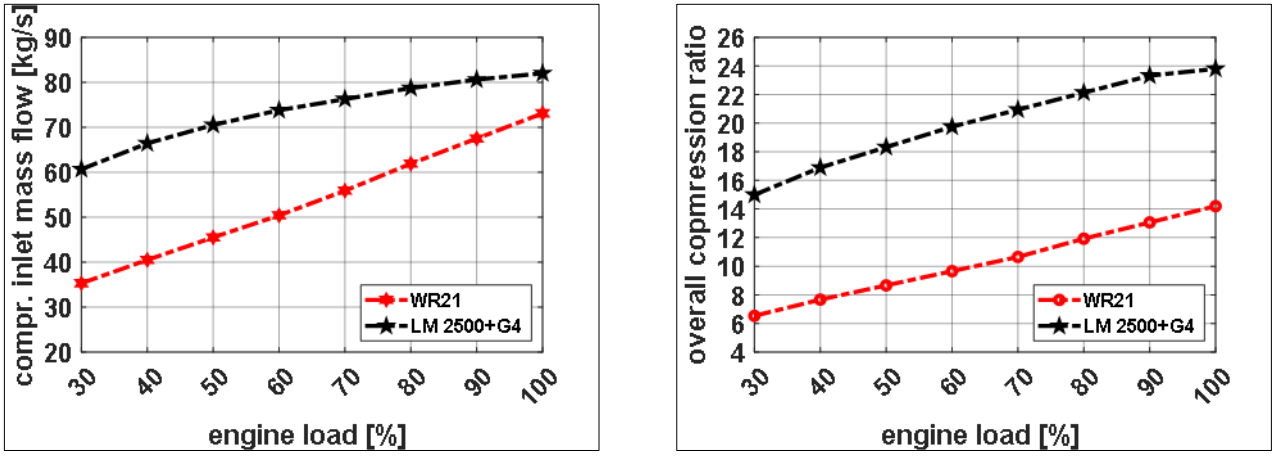

a b

Figure 7 WR21 and LM2500 GTs compressor inlet mass flow rate (a) and overall compression ratio (b) simulators results vs engines load

The GT efficiency variation to the load one, reported in Fig. 8, is very different between the two GT. In the WR21 this parameter remains almost constant between 100 and 40% MCR engine load (with a maximum at 70% one), while LM2500 efficiency always decrease to the load one. In the LM2500 the efficiency reduction in parallel to that of the GT load in typical of the GTs, the fact that this does not occur in the WR21, in a wide range of GT load variation, confirm the validity of the design choice for this GT, expressed designed to obtain these results, which is very important in the GT application as prime mover in the ship propulsion plant.

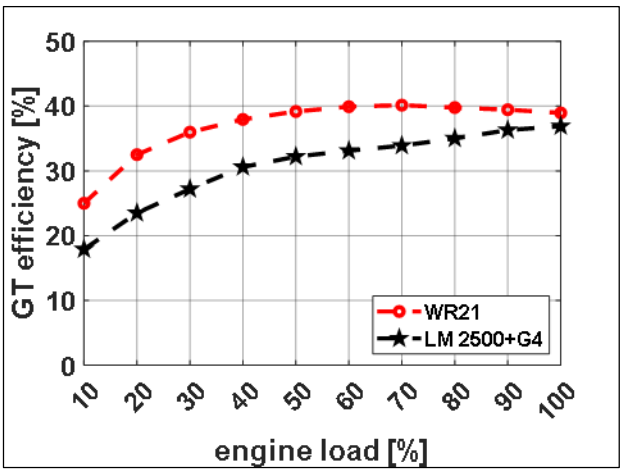

Figure 8 WR21 and LM2500 GT efficiency simulators results vs engines load

Nomenclature

- BSFC: brake specific fuel consumption
- Co: combustor
- c_p: constant pressure specific heat
- c_v: constant volume specific heat
- *f, f':* functions
- HP: high pressure
- HPc: high pressure compressor
- HP_T: high pressure turbine

- *H:* specific enthalpy
- INT: intercooler
- *J:* rotor inertia
- *K:* constant
- ICR: InterCooler Recuperated
- *LHV:* fuel lower heating
- LPc: low pressure compressor
- $LP_{T:}$ low pressure turbine
- *BFSC:* brake specific fuel consumption
- *M:* mass flow rate
- *n:* shaft speed
- *P:* power
- $P_{T:}$ power turbine
- *p:* pressure
- *Q:* shaft torque
- REG: regenerator heat exchanger
- *T:* temperature
- *t:* time
- *u:* specific internal energy
- *V:* GT component volume
- VAN : power turbine variable area nozzle
- β : compressor pressure ratio
- *Δ:* difference
- *γ:* ratio of specific heat
- *η:* efficiency
- *ε:* turbine pressure ratio, heat exchanger efficiency
- ρ: density
- 1: low pressure compressor inlet
- 2 : low pressure compressor outlet
- 3: high pressure compressor inlet
- 4: high pressure compressor outlet
- 4' : combustor inlet
- 5: combustor outlet
- 6: high pressure turbine outlet
- 7: low pressure turbine outlet
- 8: power turbine outlet
- 9: recuperator exhaust gas outlet

Subscripts

- *b:* burning
- *br:* brake
- *C:* compressor
- *cb:* combustor
- *f:* fuel
- g: gas
- *i:* inlet
- *in:* GT inlet duct
- *loss* loss
- *o:* outlet
- *nd:* non-dimensional

- *ref:* reference
- *T:* turbine

6. Conclusions

In the paper is presented an original modular simulator of the sophisticated gas turbine WR21-ICR, specifically designed for vessel propulsion plants. In the article is reported a detailed GT overall model and its components (i.e. compressors, turbines, heat exchangers, VAN and its governor) simulation description. The validation of the developed WR21-ICR GT simulator, carried out by comparing the mathematical model results with reference data, shows the model validity in the GT and its components performance determination in both design and off-design working conditions.

The comparison between the WR21 GT simulated performances with those of the currently most used GT in marine propulsion plants (LM2500), reported and commented in the article, demonstrates the WR21 GT superior performance, compared to LM2500 one, in design working conditions, but especially in off-design one. The detailed GTs performance comparison and analysis, reported in the paper, is made possible by the detailed modelling of the two GTs, the WR21-ICR carried out with the model here described, the LM2500 by an author's simulator, already presented and validated in a previous paper.

Compliance with ethical standards

Disclosure of conflict of interest

The authors declare no conflict of interest.

References

[1] Merz C A, Pakula T J. The design and operational characteristics of a combined cycle marine powerplant. ASME. 72-GT-90, V001T01A089, 13 pages, 1972 International Gas Turbine and Fluids Engineering Conference and Products Show of Turbo Expo: Power for Land, Sea, and Air, 1972. doi:10.1115/72-GT-90.

[2] Mills R G. Greater ship capability with combined-cycle machinery, Naval Engineers Journal, Vol. 89, Number 5, p. 17-8, October 1, 1977. doi.org/10.1111/j.1559-3584.1977.tb04240.x.

[3] Brady E. F. Energy conservation for propulsion of naval vessels, Naval Engineers Journal, 93, p. 131-14, 1981.

[4] Halkola J T, Campbell A H, Jung D. RACER Conceptual Design. J. Eng. Power 105(3), p. 621-6, 1983.

[5] Haglind F. A review on the use of gas and steam turbine combined cycles as prime movers for large ships. part ii: Previous work and implications. Energy Convers. Management. 49 (2008), p. 3468–7.

[6] Benvenuto G, Campora U, Laviola M. Assessment of steam cycle layouts for cogas ship propulsion systems. Proceedings of the 2th International Conference on Maritime Technology and Engineering (2014), p. 743–12.

[7] Ahlqvist I. Increasing availability through introduction of redundancy - electric propulsion. The Institute of Marine Engineers, October 5–6, 1995.

[8] Shipping World and Shipbuilder, Gas turbine system integration, Ship World Shipbuild, p. 203-11, 2002.

[9] Royal Academy of Engineering: Future ship powering options – Exploring alternative methods of ship propulsion, Report, July 2013.

[10] Smith D L, Stammetti V A. Comparative Controller design for a marine gas turbine propulsion system. Transactions ASME, J. Eng. Gas Turbines Power. Apr 1990, 112(2), Vol 122, p. 182-5, April 1990. https://doi.org/10.1115/1.2906159.

[11] Altosole M, Benvenuto G, Figari M, Campora U, Bagnasco A, D'Arco S, Giuliano M, Giuffra V, Spadoni A, Zanichelli A, Michetti S, Ratto M. Real time simulation of the propulsion plant dynamic behaviour of the aircraft carrier "Cavour". Conference Proceedings of the Institute of Marine Engineering, Science and Technology - INEC 2008: Embracing the Future, 2008.

[12] Sampath S. Fault diagnostics for advanced cycle marine gas turbine using genetic algorithms. PhD thesis. Cranfield University, United Kingdom, 2004.

[13] Bonet M U, Pilidis P. Comparative Assessment of Two Thermodynamic Cycles of an aero-derivative Marine Gas Turbine. IOSR Journal of Mechanical and Civil Engineering (IOSR-JMCE), Volume 6, Issue 3, May - June 2013, pp 76-6. ISSN: 2320-334X.

[14] North R P, Dawson R E. The design and initial development of a combustion system for the WR21 Intercooled Recuperated Gas Turbine. International Gas Turbine and Aeroengine Congress and Exposition. Houston, Texas - June 5-8,1995, ASME paper 95-GT-361.

[15] Benvenuto G, Campora U. A Gas Turbine Modular Model for Ship Propulsion Studies. HSMV, 7th Symposium on High Speed Marine Vehicles, Naples, Italy, September 21-23, 2005.

[16] Cox J C, Hutchinson D, Oswald I. The Westinghouse/Rolls-Royce WR21 Gas Turbine Variable Area Power Turbine Design. International Gas Turbine and Aeroengine Congress and Exposition. Houston, Texas, June 5-8,1995, ASME paper 95-GT-54.

[17] Sellers J and Teren F. Generalised Dynamic Engine Simulation Techniques for the Digital Computer. AGARD-CP-151, 1974.

[18] Saravanamuttoo H I H, and Mac Isaac B D. Aerothermodynamic Factors Governing the Response Rate of a Gas Turbine. AGARD-CP-151, 1974.

[19] Cottingon R V. Total Powerplant Simulation. AGARD-CP-151, 1974.

[20] Dotto A, Satta F, Campora U. Energy, environmental and economic investigations of cruise ships powered by alternative fuels. Energy Conversion and Management, 285 (2023) 117011, Elsevier (ed), 0196-8904, pp.1-18, available on: https://doi.org/10.1016/j.enconman.2023.117011.

[21] Benson R S and Whiteouse N D. Internal Combustion Engines. Pregamon Press International Library, Oxford, England, 1979.

[22] Cohen H, Rogers G F C and Saravanamuttoo H I H. Gas Turbine Theory. (Third Edition), Longman Scientific & Technical, Harlow, Essex, England, 1987.

[23] Shepard S B, Browen T L, Chiprich J M. Design and Development of the WR21 Intercooler Recuperated (ICR) Marine Gas Turbine. Transaction of the ASME, Journal of Engineering for Gas Turbines and Power, Vol. 117, July 1995, p. 557-6.

[24] Cox J C, Hutchinson D, Oswald J D. The Westinghouse/Rolls-Royce WR-21 Gas Turbine Variable Area Power Turbine Design. International Gas Turbine and Aeroengine Congress and Exposition, ASME Congress, Houston, Texas, USA, June 5-8, 1995, paper 95-GT-54.

[25] Qiu C, Song H F, Wang Y H and Huang M H. Performance estimation of variable geometry turbines. Proc. IMechE Vol. 223 Part A: J. Power and Energy, JPE714, January 27, 2009, p. 441-9, DOI: 10.1243/09576509JPE714.

[26] Anthony J C, Michael L P. Overview of the WR21 Intercooled Recuperated Gas Turbine Engine System. A modern engine for a modern fleet, International Gas Turbine and Aeroengine Congress and Exposition, ASME Congress, Cincinnati, Ohio, USA, May 24-27, 1993, paper N° 93-GT-231.

[27] Stossier W, Stauffer M, Perkins G E. WR-21 Recuperator Core Test. International Gas Turbine & Aeroengine Congress & Exibition, ASME Congress, Orlando, Florida, USA, June 2-5, 1997, paper N° 97-GT-514.

[28] Della Volpe R. Impianti Motori per la Pro, 2007, ISBN: 978-88-207-1760-5. pulsione Navale. Liguori Editore, 4th Edition, Naple, Italy.

[29] Hou Y. Cycle analysis of intercooled and regenerative naval gas turbine. Master of Engineering Thesis, Ottawa-Carleton Institute of Mechanical and Aerospace Engineering, Department of Mechanical and Aerospace Engineering, Carleton University, Ottawa, Ontario, Canada, August, 1993.